ENCIT 2018

ABCM Associação Brasileira de Engenharia e Ciências Mecânicas

17th Brazilian Congress of Thermal Sciences and Engineering
November 25th-28th, 2018, Águas de Lindóia, SP, Brazil

ENCIT-2018-0233
TOWARDS A QUALITATIVE CRITERIA FOR THE ONSET OF ABSOLUTE INSTABILITY ON REVERSED-FLOW BOUNDARY-LAYER PROFILES

Mateus Peixoto Avanci
Daniel Rodríguez
Leonardo Santos de Brito Alves
Graduate Program in Mechanical Engineering (PGMEC), Universidade Federal Fluminense, Niterói, RJ, Brazil
mateuspeixoto@id.uff.br, danielrodriguez@id.uff.br, leonardo.alves@mec.uff.br

Abstract. *Absolute instability of boundary-layer velocity profiles featuring a region of reversed flow, typical of laminar separation bubbles on flat plates, is a possible route to the onset of self-sustained oscillations and vortex shedding. The critical conditions for the appearance of absolute instability have been widely studied in the literature in terms of the ratio of the peak reversed flow with the free-stream velocity, but results also suggest that the wall-normal extent of the recirculating flow and the location of the inflection point can be of importance. This work aims at proposing a qualitative criterion for the onset of absolute instability, that depends only on the relative locations of the inflection point and the separation line.*

Keywords: *Laminar separation bubble, Boundary layer separation, Absolute/convective instability instability*

1. INTRODUCTION

Flow separation has an important impact on different technological applications. In case of airfoils, occurring as the angle of attack is increased can cause important deviations of the lift vs. angle of attack curve, leading to an increase in the drag for the same flight condition. Failure of the detached boundary layer to reattach within a short distance from the separation point usually implies a sudden loss of lift and the appearance of important pitching moments, conditions known as stall. Separation bubbles are generates primarily in applications involving low Reynolds number flows with large pressure gradients. In other technological applications, the study of low-Reynolds-number aerodynamics has increased in importance because of the development of small unmanned air vehicles (UAVs) and micro air vehicles (MAVs). Finale, flow separation at wind turbines has a prejudicial impact on the aerodynamic properties.

A laminar boundary layer separates when exposed to an sufficiently adverse pressure gradient, for example near the leading edge of the airfoil. The separated shear layer undergoes a transition due to an amplification of the flow disturbances. The resulting turbulent shear layer recalls a downstream distance resulting in the formation of a closed region commonly referred to as laminar separation bubble. If the Reynolds number is low enough the boundary layer at separation is laminar. The separated shear layer is known to be highly unstable with respect to the inflectional Kelvin-Helmholtz mechanism, and eventually transitions from the laminar to the turbulent regime.

Experimental works such as Nakano *et al.* (2007) and Zhang *et al.* (2008) have shown that the presence of separation bubbles is generally considered a negative factor since they impact aerodynamic efficiency and the behavior of the airfoil stall condition. The length of the bubble in the direction of flow increases with the angle of attack or with the reduction of the free-stream velocity, and under certain circumstances the separated shear layer may abruptly fail to re-collapse; the short bubble then suffers the so-called burst, and a long bubble forms. Unlike short bubbles, a long bubble is associated with large and potential aerodynamic effects, such as loss of lift.

Many papers focused on determining the physical causes of so-called bursting. One of the first ones was Tani (1964) and Gaster (1967) that established as the first parameter a Reynolds number based on the momentum thickness of the boundary layer in the separation. In this sense Gaster (1967) proposed a second parameter considering a inviscid pressure distribution in the bubble region. These two parameters provided a first theoretical study for the existence of bursting. Years later Pauley *et al.* (1990) refined this information by establishing a value for the pressure gradient proposed by Gaster (1967) and further suggested that the origin of vortex mats in the back of the laminar separation bubble is related to a change from convective to absolute of inflexional instability, which could be an indication for bursting. Currently this relationship with bursting has already been refuted by Marxen and Henningson (2011) and Serna and Lázaro (2015), but the absolute instability of boundary layer velocity profiles with a reverse flow region of a self excited instability has been received attention since then.

One such a possible mechanism is the inflectional instability itself, if the bubble's reversed flow portion is intense enough to sustain absolute instability, i.e. temporal growth of upstream-propagating disturbance waves. Different studies in the past analyzed this possibility. Allen and Riley (1995) described an investigation into the properties associated with small, two-dimensional separation bubbles. For such bubbles, laminar flow separation is not accompanied by laminar reattachment if the Reynolds number is sufficiently high. In that case, if reattachment is to take place, it must be as a turbulent flow. One of the main aims of this investigation is to determine the mechanism by which transition to turbulence may take place, in separated flows of such small extent, when the flow is subjected to a wall disturbance localized in time and space. However, they concluded that recirculation regions more intense than the ones present in their calculations were required for absolute instability to appear. Using modified Falkner-Skan velocity profiles with reversed flow, Hammond and Redekopp (1998) examined a family of profiles in order to analyzed for the onset of absolute instability as the magnitude of the reversed flow increase, concluding that recirculations of at least 30% of the free-stream velocity were required. Another work of interest is Rist and Maucher (2002), which focuses on the analysis of parameters as wall distance of the inflection point, intensity of the shear layer, reverse-flow velocity and local Reynolds number in a possible absolute instability within a temporal instability approach; they lower the threshold for absolute instability to 30% of the free-stream velocity. More recently Diwan (2009) studied the dynamics of early stages of transition associated with laminar separation bubbles from a combined experimental and theoretical approach. He further reduced the reversed-flow threshold for absolute instability to a smaller 16%. Finally, Rodríguez *et al.* (2013) studied a family of LSB flows with peak reversed flows lower than 13% concluding that no absolute inflectional instability was present for the bubbles considered, while a three-dimensional stationary instability was already active for peak reversed flows as low as 7%, suggesting a different transition mode.

All the referenced studies considered different families of base flows and even if they allowed for variations in the wall-normal extent of the reversed flow region, they concentrated their analyses on the peak reversed flow. This opens the possibility of an even reduced critical reversed flow for self-sustained instability if the wall-normal extent of the bubble is varied appropriately. The present study starts from a inviscid analysis with Rayleigh's equation and a hyperbolic tangent velocity profile such a Dovgal *et al.* (1994); Alam and Sandham (2000); Niew (1993) and a piecewise linear profile. The analytic profile is used to construct generic models of separation bubbles and study the possible onset of local absolute instability in the representative spatially-developing flows in order to verify whether or not the peak recirculation is the only parameter of interest.

2. METHODOLOGY

2.1 Linear Stability Theory

The calculations are based on the usual assumptions for Linear Stability Theory of incompressible fluids: parallel-flow approximation, small-amplitude disturbances and normal disturbance modes, i.e., a decomposition of the total flow-field as Eq. (1).

$$\mathbf{q}(x,y,t) = \bar{\mathbf{q}}(y) + \epsilon \mathbf{q}'(x,y,t) \tag{1}$$

Here $\bar{\mathbf{q}}(y) = \bar{u}(u)$ is the base flow profile, $\mathbf{q}'(x,y,t) = [u', v', p']^T$ is the vector of disturbance fluid variables, ϵ is the linearly-small disturbance amplitude, x is the streamwise coordinate, y is the wall-normal coordinate and t is time.

2.2 Orr-Sommerfeld/Rayleigh

To theoretically investigate stability characteristics of locally-parallel LSB profiles, modal analyses using both the Orr-Sommerfeld and Rayleigh equations have been performed. The Orr–Sommerfeld equation is an eigenvalue equation describing the viscous linear two-dimensional instability modes of a parallel flow and it is given by Eq. (2). See Drazin and Reid (2004).

$$\left(\bar{u} - \frac{\omega}{\alpha}\right)\left(\phi'' - \alpha^2\phi\right) - U''\phi = \frac{1}{\mathrm{i}\alpha Re}\left(\phi^{iv} - 2\alpha^2\phi'' + \alpha^4\phi\right) \tag{2}$$

The prime (') indicates differentiation with respect to y. All the quantities are non- dimensionalized using appropriate parameters. Thus, α is a streamwise wave number and ω is a the complex frequency, Re is the Reynolds number and i the imaginary number. $\phi(y)$ is the complex amplitude of the disturbance streamfunction which is directly proportional to the transverse disturbance velocity v, and is related to the streamwise disturbance velocity by

$$u(x,y,t) = -\frac{1}{\mathrm{i}\alpha}\phi(y)e^{\mathrm{i}(\alpha x - \omega t)} + c.c. \tag{3}$$

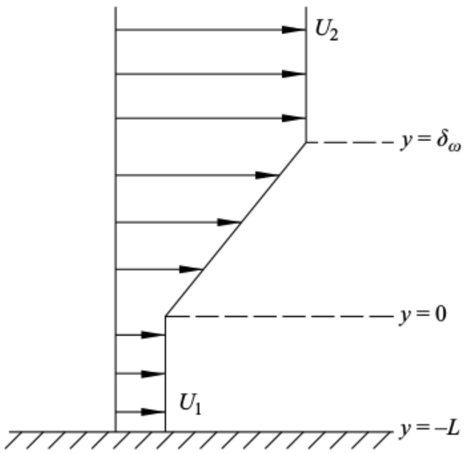

Figure 1: Three-piece linear profile in the presence of wall, Diwan and Ramesh (2009)

The inviscid Kelvin-Helmholtz instability being dominant for LSBs, the simpler Rayleigh's equation is expected to deliver results comparable to those of the complete Orr-Sommerfeld equation for this class of base flows. Rayleigh's equation is obtained by neglecting the viscous term in the Orr-Sommerfeld's equation, Eq. (2), and is given by Eq. (4).

$$\left(U - \frac{\omega}{\alpha}\right)\left(\phi'' - \alpha^2\phi\right) - U''\phi = 0 \tag{4}$$

The simpler form of Rayleigh's equation allows us to perform a large parametric study in a reasonable time.

2.3 Three different families of profiles with reversed flow

The first modified hyperbolic tangent profile was proposed by Dovgal *et al.* (1994) is used here to construct a wide variety of base flows representative of LSBs:

$$\bar{u}(y) = [\tanh(a(y-d)) + \tanh(ad)]/(1+\tanh(ad)) + b\sqrt{3}(y/d)exp[-1.5(y/d)^2 + 0.5] \tag{5}$$

Here b is a measure of the magnitude of reversed flow and d is the non- dimensional distance of the inflection point from the wall. The constant a is chosen such that the momentum thickness is equal to one, i.e. Eq. (6) is satisfied.

$$\int_0^\infty U(y)(1-U(y))dy = 1 \tag{6}$$

The second modified hyperbolic tangent profile was proposed by Alam and Sandham (2000):

$$\bar{u}(y) = \tanh(y) - 2A\frac{\tanh(y/B)}{\cosh^2(y/B)} \tag{7}$$

In this profile A and B are constants which can be adjusted to fit particular profiles from the numerical simulations or used for parametric studies which is the case of this work.

The third and last one modified hyperbolic tangent profile was proposed by Niew (1993):

$$\bar{u}(y) = \frac{\tanh(Ay)(\tanh(Ay-B)+C)}{1+C} \tag{8}$$

In this case the constant A is associated with the value of the shear $du_{analytic}/dy$, the constant B regulates the distance of the shear layer from the wall and the constant C defines the amount of the reverse flow.

2.4 Piecewise linear profile

The previous profiles considered realistic profiles, that have been used in the literature to approximate those from experimental or numerical simulations. The simpler definition of the base flow allows for a great flexibility in the multi-parametric range to be studied (see Fig. 1), while retaining the main quantities characterizing the separated flow. Additionally, the dispersion relation for instability waves is known analytically Diwan and Ramesh (2009):

$$\frac{\left[\lambda - \overline{\alpha}\frac{(1-\lambda-\overline{c})}{(1-e^{2\overline{\alpha}L/\delta_w})}\right]}{e^{\overline{\alpha}}[\overline{\alpha}(1+\lambda-\overline{c})-\lambda]} = \frac{\left[\overline{\alpha}\frac{(1-\lambda-\overline{c})e^{2\overline{\alpha}L/\delta_w}}{(1-e^{2\overline{\alpha}L/\delta_w})} - \lambda\right]}{\lambda e^{-\overline{\alpha}}} \tag{9}$$

where $\overline{\alpha} = \alpha\delta_w$; $\overline{c} = c/U_m$; $U_m = (U_1 + U_2)/2$; and $\lambda = (U_2 - U_1)/U_2 + U_1$. Unlike the previous profiles, in this case the parameters to be analyzed are the inflection point y^*_{inf} and the dividing point y^*_d. For each pair of this two parameters we got the respective pinch. The $(*)$ is because for these cases the coordinates is respect to origin $y = -L$.

2.5 Numerical methods

Two different numerical methods for the solution of the locally-parallel eigenvalue problems described by the Orr-Sommerfeld and Rayleigh's equations are employed in this work. The first one is a matrix-forming approach, used for both equations, in which the differential operators are spatially discretized using a conveniently mapped Chebyshev-Gauss-Lobatto mesh. This results into a matrix eigenvalue problem, that is formed and stored in memory and solved numerically using the implementation of the QZ algorithm available in the open-source library LAPACK, as was first done by Orszag (1971).

The second method is based on the spatial marching of the governing equations from the free-stream towards the wall. For a prescribed wavenumber α, the value of ω is adjusted iteratively until the boundary conditions at the wall are satisfied. This second method, usually known as shooting method, is only used here for the solution of the inviscid Rayleigh's equation.

The results of both approaches are cross-validated for some representative cases. The matrix-forming method is also used in the comparison between viscous and inviscid analyses, in order to ascertain if viscosity plays an important role in the critical conditions for the onset of absolute instability. Finally, the matrix-forming results are also used to provide initial guesses for the shooting method, so the parametric studies can be initialized.

The determination of the absolute/convective nature of instability waves is based on the behavior of the waves with zero group velocity, i.e. $\frac{\partial\omega}{\partial\alpha} = 0$, as those waves do not propagate either upstream or downstream from their location of introduction. The zero group velocity condition is a saddle-point condition for the complex ω in the complex α plane, and its determination can be done following different approaches. Based on the results of the matrix-forming approach, a rectangular mesh in the α plane is mapped onto the ω plane, and the zero-group-velocity conditions are identified visually where the coordinate lines fold intersecting themselves into a cusp-point. Corresponding to this complex ω_0, a saddle point is identified in the α plane, in which two branch solutions, α^+ and α^- intersect themselves in a saddle or pinching point. This procedure is tedious and not advisable for a large parametric study, as the one intended here; consequently a different and novel approach is used instead, described in the next section, and the one based on the identification of the cusp point is employed only for cross validations and providing the initial guesses.

2.6 Shooting method to determine pinch-point

The idea here is transform the boundary condition problem in a initial condition problem and solve a system of two complex equations that determine the dispersion relation involving the four variables α_r, α_i, ω_r and ω_i. Rayleigh's equation (4) is the first governing equation; a convenient second equation is obtained by differentiating Rayleigh's equation with respect to α:

$$\left[\left(U - \frac{\partial\omega}{\partial\alpha}\right)(\phi'' - \alpha^2) - 2\alpha(\alpha U - \omega) - U''\right]\phi + [(\alpha U - \omega)(\phi'' - \alpha^2) - \alpha U_{yy})]\phi_\alpha = 0, \tag{10}$$

where ϕ_α is $\frac{\partial\phi}{\partial\alpha}$. With the objective of restricting the possible solutions to those with zero group velocity, $\frac{\partial\omega}{\partial\alpha} = 0$ is imposed implicitly in Eq. (10).

The system of equations is solved using a shooting method, marching from the free-stream towards the wall. "Initial" free-stream conditions need to be imposed to the real and imaginary parts of ϕ and ϕ_α, as well to their first derivatives:

$$\phi_\infty = 1, \quad \phi'_\infty = -i\alpha, \quad \phi_{\alpha\infty} = 0 \quad \text{and} \quad \phi'_{\alpha\infty} = -i. \tag{11}$$

The complex α and ω values are iterated with the aid of a Newton's method until the "final" wall conditions are satisfied:

$$Re(\phi_0) = 0, \quad Im(\phi_0) = 0, \quad Re(\phi_{\alpha 0}) = 0 \quad \text{and} \quad Im(\phi_{\alpha 0}) = 0. \tag{12}$$

The computed solutions verify Rayleigh's equation and boundary conditions and the zero-group-velocity condition, and thus corresponds automatically to saddle points in the complex α plane. The corresponding complex frequency and wavenumber are referred to as the absolute frequency ω_0 and the absolute wavenumber α_0. If the imaginary part of the absolute frequency is positive, then instability waves exist which grow in amplitude while they propagate upstream, i.e. the base flow profile is absolute unstable. Consequently, $Im(\omega_0) = 0$ determines the critical conditions for the onset of absolute instability.

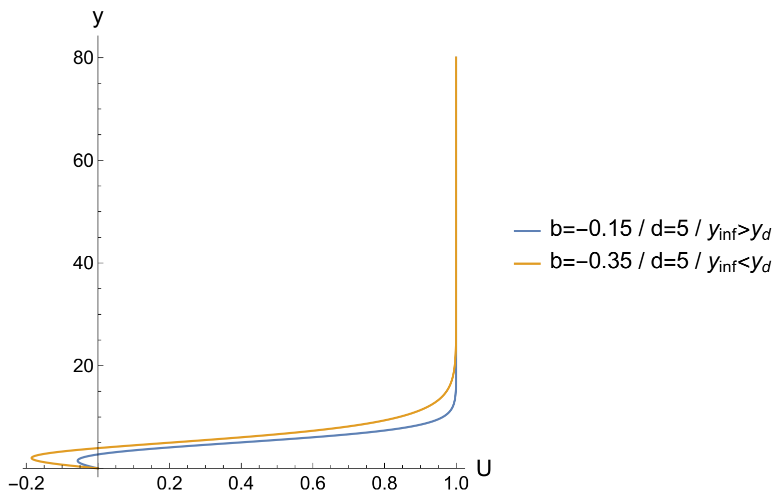

Figure 2: Two base flow profiles are showing following Dovgal *et al.* (1994).

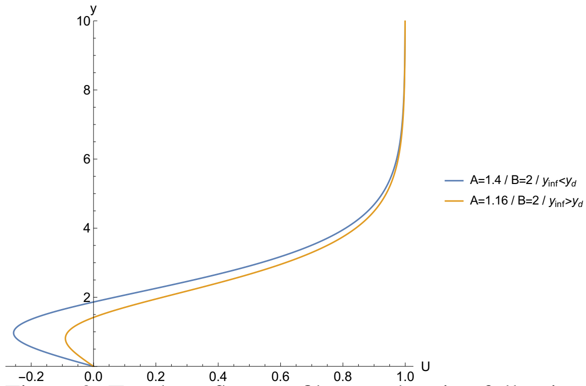

Figure 3: Two base flow profiles are showing following Alam and Sandham (2000).

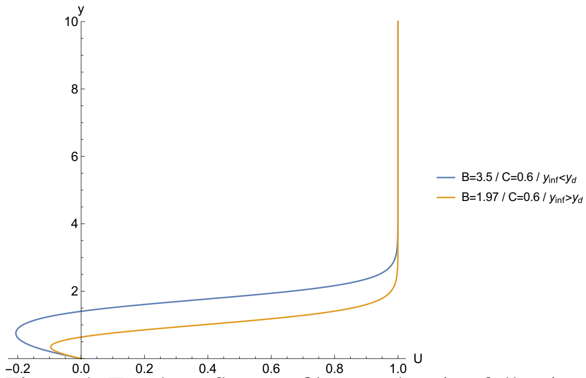

Figure 4: Two base flow profiles are showing following Niew (1993).

3. RESULTS

3.1 Description of the cases and additional cross-validations

In order to characterize the analytical solution for the base flow profile, two cases examples for each tangent hyperbolic profiles are presented in Fig. 2, 3 and 4. One of them has a inflection point coordinate y_{inf} lower than that of the dividing point y_d, and the other base flow profile the contrary.

3.2 Absolute/Convective analyses

A large parametric study of the absolute frequency for varying base flows was performed using the validated shooting method from section 2.6 The results are shown in Fig. 5, Fig. 6 and Fig. 7. The same was made for the piecewise linear profile varying the value of the peak reverse flow, the results are shown in Fig. 8 and 9.

Here the red lines represents the critical curves for the convective/absolute instabilities, $Im(\omega_0) = 0$. We can observe that the peak reversed flow is in good agreement with the literature (Diwan (2009); Rist and Maucher (2002)) and is about 15% if the free-stream velocity. However, these results show that the reversed flow is not enough to determine if the configuration is convectively or absolutely unstable, and the wall-normal size of the reversed flow region, h_R, also must be taken into account. For the piecewise linear profiles we can observe two critical curves. We have to consider just one of then because this analysis is for positive values of alpha to satisfy the boundary conditions and for this reason just one critical curve is valid.

3.3 Dividing/Inflection point

In possession of the results the next step was mapping the pinch-points with the related inflection and dividing points for the hyperbolic tangent profiles.

In order to establish a relation between y_{inf}, y_d and the onset of the absolute instability we can plot the critical curve

($\omega_i = 0$) with respect to these parameters, which is shown in Fig. 10. The results show that for values $y_{inf} > y_d$ the inflectional instability is of convective nature, while for $y_{inf} < y_d$ absolute instability is recovered in all cases. For the piecewise linear profiles we can show the analog figure, Fig. 11 but now with more values of peak reverse flow. For these profiles the curves diverge from the criterion we are proposing. We consider this to be because these profiles do not really get a inflection point and we are using an approximation to it $y_{inf} = \delta_w/2$.

4. CONCLUSIONS

This paper addresses a qualitative criteria for the onset of absolute instability by means of locally-parallel linear stability analyses of velocity profiles representative of boundary layers with reversed flow and a piecewise linear profile.

Present results, considering three different families of boundary-layer profiles with separation, show that the critical conditions for absolute instability are not solely dependent on the peak reversed flow, but also on the wall-normal extent of the reversed flow region. In the literature corresponds the threshold is about 16$\%$ which give us an upper bound, and for the analyzed profiles this can vary between 12-15$\%$.

Following a suggestion made by Diwan (2009), the relation between the absolute/convective instability and the relative coordinates of the base flow's inflection point and dividing streamline is monitored. For the tangent hyperbolic profiles is found that when the inflection point lies within the reversed flow region, absolute instability should be expected, while an inflection point outside implies convective instability. Considering the linear piecewise profiles the criterion diverges with the value of peak reverse flow. It is because these profiles is the most simple way to describe a laminar separation bubble profile with reverse flow without a inflection point properly. For future studies this can be investigate varying this evaluation.

5. ACKNOWLEDGEMENTS

The first author's work is funded by a CAPES post-graduate scholarship, within the Postgraduate program in Mechanical Engineering (PGMEC/UFF). This work is supported by CNPq (grants 405144/2016-4, 305512/2016-1) and FAPERJ (grants 200003, 223669).

6. REFERENCES

Alam, M. and Sandham, N.D., 2000. "Direct numerical simulation of 'short'laminar separation bubbles with turbulent reattachment". *Journal of Fluid Mechanics*, Vol. 410, pp. 1–28.

Allen, T. and Riley, N., 1995. "Absolute and convective instabilities in separation bubbles". *The Aeronautical Journal*, Vol. 99, No. 990, pp. 439–449.

Diwan, S.S. and Ramesh, O., 2009. "On the origin of the inflectional instability of a laminar separation bubble". *Journal of Fluid Mechanics*, Vol. 629, pp. 263–298.

Diwan, S., 2009. *Dynamics of early stages of transition in a laminar separation bubble*. Ph.D. thesis, PhD thesis, Indian Institute of Science, Bangalore, India.

Dovgal, A., Kozlov, V. and Michalke, A., 1994. "Laminar boundary layer separation: instability and associated phenomena". *Progress in Aerospace Sciences*, Vol. 30, No. 1, pp. 61–94.

Drazin, P.G. and Reid, W.H., 2004. *Hydrodynamic stability*. Cambridge university press.

Gaster, M., 1967. "The structure and behaviour of separation bubbles, arcr &m".

Hammond, D.A. and Redekopp, L.G., 1998. "Local and global instability properties of separation bubbles". *European Journal of Mechanics-B/Fluids*, Vol. 17, No. 2, pp. 145–164.

Marxen, O. and Henningson, D.S., 2011. "The effect of small-amplitude convective disturbances on the size and bursting of a laminar separation bubble". *Journal of Fluid Mechanics*, Vol. 671, pp. 1–33.

Nakano, T., Fujisawa, N., Oguma, Y., Takagi, Y. and Lee, S., 2007. "Experimental study on flow and noise characteristics of naca0018 airfoil". *Journal of Wind Engineering and Industrial Aerodynamics*, Vol. 95, No. 7, pp. 511–531.

Niew, T.R., 1993. "The stability of the flow in a laminar separation bubble". *NASA STI/Recon Technical Report N*, Vol. 95.

Orszag, S.A., 1971. "Accurate solution of the orr–sommerfeld stability equation". *Journal of Fluid Mechanics*, Vol. 50, No. 4, pp. 689–703.

Pauley, L.L., Moin, P. and Reynolds, W.C., 1990. "The structure of two-dimensional separation". *Journal of Fluid Mechanics*, Vol. 220, pp. 397–411.

Rist, U. and Maucher, U., 2002. "Investigations of time-growing instabilities in laminar separation bubbles". *European Journal of Mechanics-B/Fluids*, Vol. 21, No. 5, pp. 495–509.

Rodríguez, D., Gennaro, E.M. and Juniper, M.P., 2013. "The two classes of primary modal instability in laminar separation bubbles". *Journal of Fluid Mechanics*, Vol. 734.

Serna, J. and Lázaro, B., 2015. "On the bursting condition for transitional separation bubbles". *Aerospace Science and Technology*, Vol. 44, pp. 43–50.

Tani, I., 1964. "Low-speed flows involving bubble separations". *Progress in Aerospace Sciences*, Vol. 5, pp. 70–103.

Zhang, W., Hain, R. and Kähler, C.J., 2008. "Scanning piv investigation of the laminar separation bubble on a sd7003 airfoil". *Experiments in Fluids*, Vol. 45, No. 4, pp. 725–743.

7. RESPONSIBILITY NOTICE

The author(s) is (are) the only responsible for the printed material included in this paper.

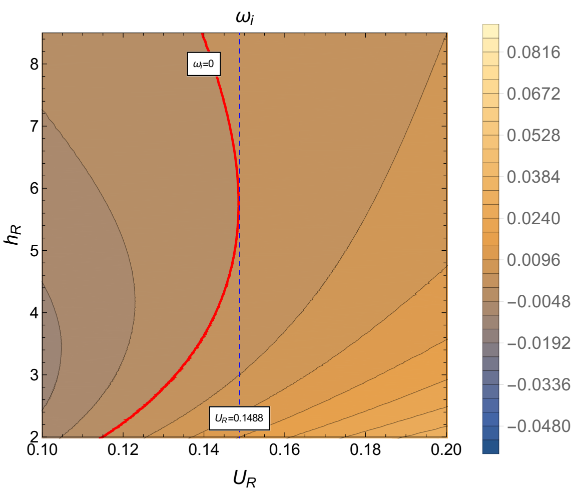

Figure 5: Variation of ω_i with the parameters U_R and h_R, Dovgal *et al.* (1994) profile.

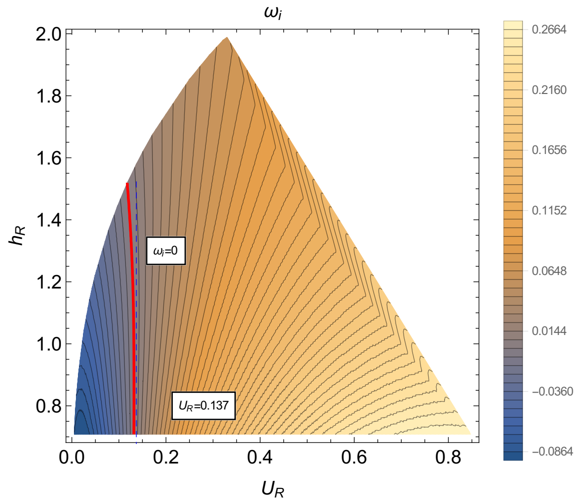

Figure 6: Variation of ω_i with the parameters U_R and h_R, Alam and Sandham (2000) profile.

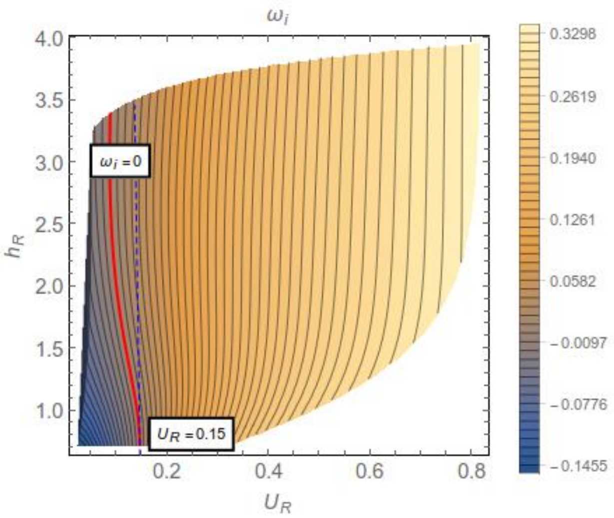

Figure 7: Variation of ω_i with the parameters U_R and h_R, Niew (1993) profile.

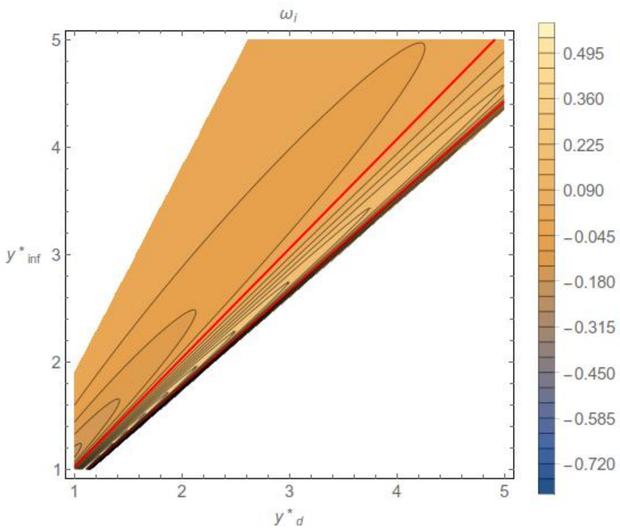

Figure 8: Variation of ω_i with the parameters y^*_{inf} and y^*_d. $U_R = 15\%$

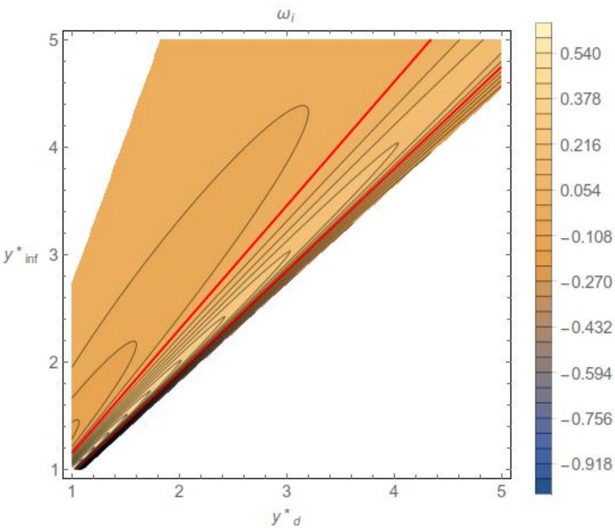

Figure 9: Variation of ω_i with the parameters y^*_{inf} and y^*_d. $U_R = 10\%$

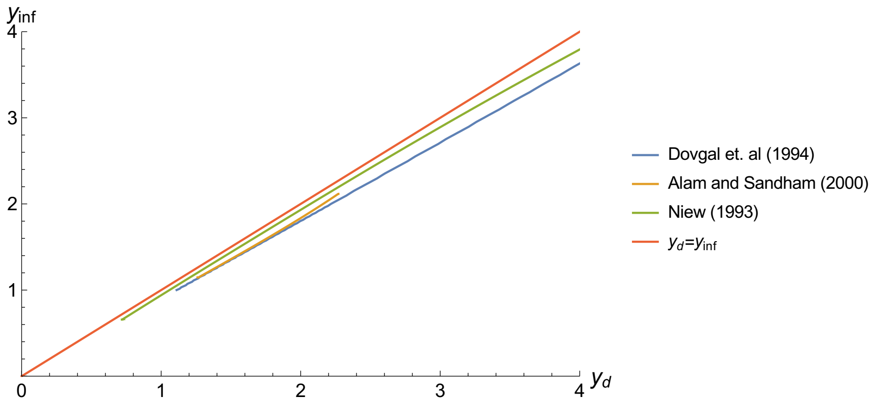

Figure 10: The critical curve ($\omega_i = 0$) with the variation of y_{inf} and y_d.

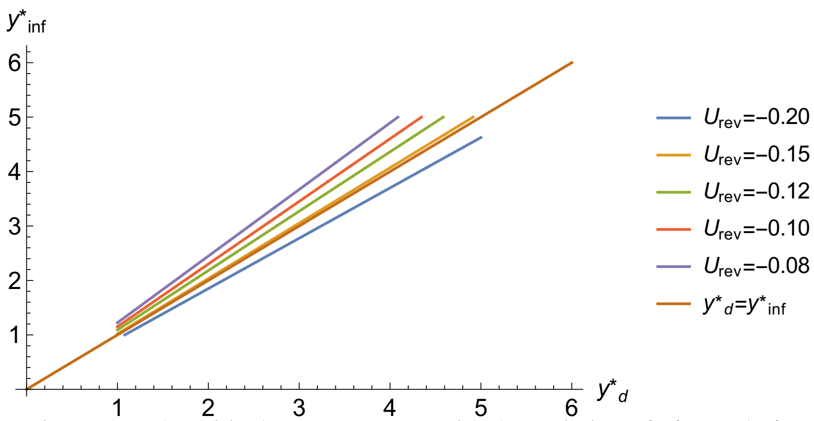

Figure 11: The critical curve ($\omega_i = 0$) with the variation of y^*_{inf} and y^*_d.